RAPID COMMUNICATIONS

PHYSICAL REVIEW B VOLUME 44, NUMBER 12 15 SEPTEMBER 1991-II

Rapid Communications

Rapid Communications are intended for the accelerated publication of important new results and are therefore given priority treatment both in the editorial office and in production. A Rapid Communication in **Physical Review B** *should be no longer than 4 printed pages and must be accompanied by an abstract. Page proofs are sent to authors.*

Roles of band states and two-photon transitions in the electroabsorption of a polydiacetylene

Y. Kawabe,* F. Jarka, and N. Peygambarian
Optical Sciences Center, University of Arizona, Tucson, Arizona 85721

D. Guo and S. Mazumdar
Department of Physics, University of Arizona, Tucson, Arizona 85721

S. N. Dixit
Lawrence Livermore National Laboratories, Livermore, California 94550

F. Kajzar
Commisariat à l'Énergie Atomique, Institut de Recherche Technologique et de Développment Industriel de la Commissariat à l'Énergie Atomique, Laboratoire de Physique Electronique des Materiaux, Centre d'Etudes Nucléaires de Saclay, F-91191 Gif-sur-yvette CEDEX, France

(Received 15 April 1991)

We report results of experimental and theoretical investigations of electroabsorption (EA) in a poly[1,6-di(*N*-carbazolyl)-2,4-hexadiyne] DCH polydiacetylene. In addition to the Stark shift of the exciton, a high-energy feature is seen in EA, whose origin has been the subject of controversy. Based on exact theoretical calculation of the EA within an extended Peierls-Hubbard model, we ascribe the high-energy signal to transitions to a continuum threshold. We briefly discuss the contributions of these band threshold states to the third-order optical nonlinearity, $\chi^{(3)}$.

Organic conjugated polymers with large optical nonlinearities and short excited-state relaxation times have generated considerable interest.[1] Recent work by several different groups[2-4] already suggests potential practical uses. Design of practical nonlinear optical devices would require detailed knowledge of the electronic structures of these materials. Significant progress in the fabrication of oriented organic films of high optical quality,[5,6] as well as in the theoretical description beyond single-particle approaches,[7] has greatly increased our understanding of the low-energy (below gap) excitations in these systems. Nonlinear optical response, however, can depend also on high-energy (above gap) excited states.

Eigenstates of linear conjugated polyenes and polymers with a center of inversion, such as polydiacetylenes (PDA's), are classified as A_g if they are symmetric with respect to the inversion center, and B_u if they are asymmetric. Each state is further characterized by a quantum number that gives its relative ordering, the $1A_g$ being the ground state. Dipole-allowed transitions occur only between A_g and B_u states, making excitation from the ground state to A_g states one-photon forbidden but two-photon allowed. A weak static electric field, **F**, applied parallel to the chain direction can significantly alter this description by mixing these A_g and B_u states according to

$$\psi_n = \psi_n^{(0)} + \sum_{k \neq n} \psi_k^{(0)} \frac{(H_F)_{kn}}{E_n^{(0)} - E_k^{(0)}} . \quad (1)$$

Here $H_F = \boldsymbol{\mu} \cdot \mathbf{F}$ is the perturbation due to **F**, and $\boldsymbol{\mu}$ is the dipole operator. The unperturbed $\mathbf{F}=\mathbf{0}$ wave functions and energies are denoted by $\psi_n^{(0)}$ and $E_n^{(0)}$, while ψ_n is the perturbed wave function. $(H_F)_{kn}$ are the matrix elements of H_F between the unperturbed states. Clearly, $\psi_n^{(0)}$ and $\psi_k^{(0)}$ have opposite symmetries, and ψ_n has both A_g and B_u character, the extent of the mixing being dependent on the magnitude of the field F. Thus for $F \neq 0$, previously forbidden A_g states become weakly allowed, while B_u states get suppressed and shifted.

Although previous electroabsorption (EA) studies of PDA's (Refs. 8–11) agree that the field-induced absorptions are due to the PDA backbone, interpretations of these experiments differ. Independent of side groups, a Stark shift of the optically allowed exciton absorption is accompanied by a strong signal on the high-energy side where no significant feature in linear absorption is seen. Sebastian and Weiser ascribed the origin of this signal to dipole-allowed transitions to the conduction band.[8,9] More recent work by Tokura *et al.*,[10,11] however, conclude

that this feature is due to a dipole-forbidden A_g transition. This situation becomes even more complicated when one considers the results of the electric-field-induced second-harmonic generation and third-harmonic generation (THG) in DCH-PDA. These experiments find a strong A_g state nearly degenerate with the exciton[5] and, therefore, considerably below the state seen in EA. Our work is intended to clarify the controversies surrounding the subject and to determine the roles played by high-energy dipole-allowed and dipole-forbidden states in poly[1,6-di(*N*-carbazolyl)-2,4-hexadiyne] (DCH-PDA).

In our experiment, a mono-oriented 400-Å-thin film of DCH-PDA was prepared by the vacuum evaporation method on potassium phthalate single-crystal substrate as described in Refs. 5 and 6. Observation of a strong dichroism confirmed the alignment of the molecular backbones. Coplanar aluminum electrodes with gap spacing of 50 μm were deposited by electron-beam evaporation. The optical setup included a halogen lamp, a polarizer, a monochromator with a 25-cm focal length, and a photomultiplier. The room-temperature EA measurement was performed by applying a 200-Hz rectangular unipolar electric field up to 120 kV/cm through a homemade transistor switching circuit. The electric field and the polarization direction of the monochromated light were arranged parallel to the conjugated chains of the polymer. The modulated light intensity detected by the photomultiplier was processed by a lock-in amplifier and acquired by a microcomputer.

The linear absorption spectrum, α_0, of our sample, plotted in Fig. 1(a), shows a large excitonic absorption peak at 1.85 eV accompanied by vibrational satellites.[12] While photoconductive measurements place the band edge at around 2.4 eV in PDA's,[13] the large oscillator strength of the exciton does not allow the clear appearance of the band edge in the linear absorption spectra.

In Fig. 1(b) we show the change in absorption, $\Delta\alpha$, for an electric field of 120 kV/cm. Comparison with Fig. 1(a) indicates that the differential absorption between 1.8 and 2.1 eV corresponds to a redshift of about 0.18 meV of the exciton and its vibronics. We have verified that $\Delta\alpha$ is proportional to F^2, indicating that the shift is a simple Stark effect.[8–11] In addition to the shift of the exciton, the aforementioned higher-energy signal is seen at 2.35 eV. We note that this feature is not a peak, but rather appears as an oscillatory signal, crossing the zero line several times.

In order to interpret our data, we have explicitly calculated the electroabsorption within the Peierls-extended Hubbard Hamiltonian for the half-filled band of π electrons,

$$H_0 = U\sum_i n_{i\uparrow}n_{i\downarrow} + V\sum_i (n_i - 1)(n_{i+1} - 1) + t\sum_{i,\sigma}[1 + (-1)^i\delta](c_{i\sigma}^\dagger c_{i+1,\sigma} + c_{i+1,\sigma}^\dagger c_{i\sigma}) , \quad (2)$$

where $c_{i\sigma}^\dagger$ creates an electron of spin σ at site i, $n_{i\sigma} = c_{i\sigma}^\dagger c_{i\sigma}$ is the corresponding number operator, and $n_i = \sum_\sigma n_{i\sigma}$. The matrix element t is the nearest-neighbor hopping integral, U and V are the on-site and the nearest-neighbor Coulomb repulsions between π electrons, and δ is a bond alternation parameter. For simplicity, we have retained

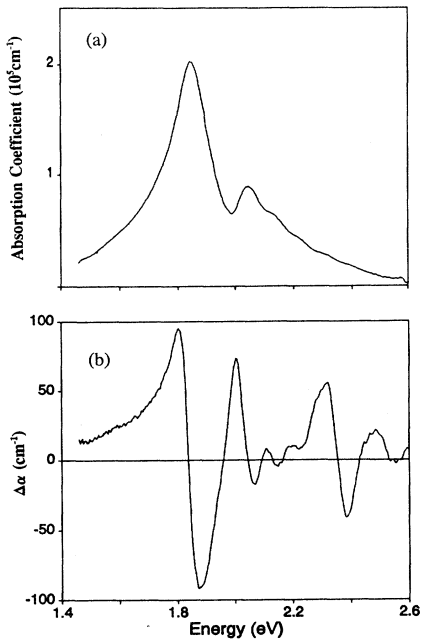

FIG. 1. (a) The measured linear absorption coefficient, $\alpha_0(\omega)$, of our DCH-PDA sample. The large excitonic peak is shown with higher-energy vibronic sidebands; (b) absorption changes, $\Delta\alpha = \alpha - \alpha_0$, for a 120-kV/cm field applied to the sample with coplanar electrodes separated by 50 μm. A Stark shift of the exciton and its vibronics is clearly seen with an additional higher-energy feature beginning at 2.35 eV.

only two alternating hopping integrals, $t(1 \pm \delta)$, as is appropriate for polyacetylene rather than for PDA's. To the best of our knowledge, no such calculation of EA exists, although calculations of second-harmonic coefficients have been done.

Our calculations are exact, but are for a finite chain of length $N = 8$. The dimension of the Hamiltonian matrix is 945 for $F \neq 0$; for $N = 10$, the dimension increases by an order of magnitude. Thus, employing a larger N for the calculation would require a considerably larger amount of effort, without giving much additional physical insight. This is because the spectrum for $N = 10$ is still discrete, thereby missing the continuum expected in an infinite chain. The well-defined exciton and a continuum at higher energy of the PDA's (Ref. 13) are qualitatively simulated in a controlled manner by doing the $N = 8$ calculations with artificially large U and V. For strong coupling, excitonic states at $U - V$ and band states at U are obtained, while for realistic coupling (smaller U, V) in finite chains, no distinction between exciton and band states can be made. For the same reason, we have neglected long-range Coulomb interactions that appear in Pariser-Parr-Pople models. Long-range interactions increase the discreteness of the spectrum in finite chains. We present results for representative U and V values only. However, we emphasize that we have examined a very large region of the U, V parameter space to confirm the universality of our results.

The EA is calculated in the following manner. Exact eigenstates and dipole moments of the field-free-extended

Hubbard Hamiltonian are first evaluated. The exact mixed states for $F \neq 0$ are then calculated by diagonalizing the total Hamiltonian in the basis space of the field-free Hamiltonian. Optical absorptions are separately calculated for the two cases of zero and nonzero field to obtain the differential absorption.

Figure 2(a) shows the zero-field linear absorption for $N=8$, $U=10$, $V=3$, and $\delta=0.1$. All parameters are in units of t, while the energies are in units of E_x, the energy of the $1B_u$ exciton. The strong peak results from the transition to the $1B_u$ exciton, and the peaks to its right correspond to higher B_u states. The differential absorption for a field of 0.005, which would correspond to about 800 kV/cm, is shown in Fig. 2(b). Since a true continuum is not obtained for $N=8$, even with large U and V, artificially large fields are required to obtain $\Delta\alpha/\alpha$ comparable to experiment. The most striking feature of Fig. 2(b) is its strong similarity to the experimental $\Delta\alpha$ spectrum.

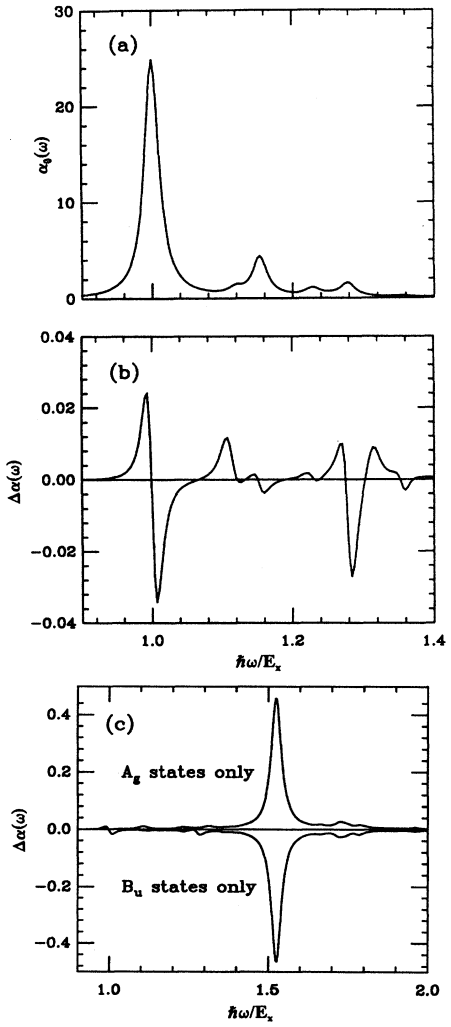

FIG. 2. (a) Calculated linear absorption in arbitrary units for the extended Hubbard Hamiltonian, $N=8$, $U=10$, $V=3$, $\delta=0.1$; (b) calculated $\Delta\alpha$ in arbitrary units for a field of $F=0.005$; (c) contributions to $\Delta\alpha$ by A_g and B_u states individually; the units are the same as in (b), but note that the scales are very different.

Contributions to $\Delta\alpha$ from A_g to B_u states are of opposite signs. The $1B_u$ exciton is perturbed by the neighboring A_g states. Dixit, Guo, and Mazumdar[14] have recently shown that dipole coupling of $1B_u$ to A_g states below[15] the exciton is weak, while strong coupling of $1B_u$ exists with an A_g state immediately above it. This A_g state above $1B_u$ is hereafter referred to as the mA_g state. Recent experiments on a different PDA by Torruellas *et al.*[16] agree with this prediction. The strong coupling with the mA_g leads to a redshift of the $1B_u$ exciton, as seen in Figs. 1(b) and 2(b). The peak at $\hbar\omega=1.1E_x$ in the theoretical $\Delta\alpha$ plot corresponds to this mA_g state. In Fig. 1(b), the signal at 2.35 eV is seen to be oscillatory in nature, and not peaklike, which clearly precludes its origin from the mA_g, or any other A_g state.

A prominent oscillatory feature in the theoretical $\Delta\alpha$ appears only at $\hbar\omega \geq 1.24E_x$, while above this threshold $\Delta\alpha$ is small again. Starting from a well-defined B_u state at this threshold, which hereafter we denote as nB_u, the zero-field dipole moments between neighboring A_g and B_u states become anomalously large. Note that α itself has a small magnitude with no structure in this energy regime. These dipole moments between states that are extremely close in energy are larger than even $\langle 1B_u|\mu|mA_g\rangle$, and are, therefore, orders of magnitude larger than dipole moments between other states below nB_u. A further characteristic of nB_u is its strong coupling to mA_g (note that mA_g is also strongly coupled to $1B_u$).

We have done several different calculations indicating that nB_u forms the lower threshold of a continuum. First, we calculated $\Delta\alpha$ due to A_g and B_u states separately at all energies. These results are shown in Fig. 2(c), where we go to energies twice the exciton energy. The EA due to the A_g and B_u states individually are giant above the nB_u, so much so that EA at lower energies is almost invisible on the scale of Fig. 2(c). Such huge $\Delta\alpha$ necessarily require states that are extremely close in energy [see Eq. (1)]. Furthermore, although the contributions to $\Delta\alpha$ due to the A_g and B_u states individually are large, the overall $\Delta\alpha$ is small compared to even the EA at lower energies. This indicates a near cancellation, which again requires levels very close to one another. Both these features indicate a pseudocontinuum at $N=8$, which would correspond to a true continuum at $N \rightarrow \infty$. A second set of calculations confirming the nature of nB_u required the variation of U and V. The nB_u in each case was identified from dipole moment calculations. For each U, nB_u was the lowest state whose energy was independent of V, while energies of states below nB_u increased linearly with $U-V$. By varying U, we then confirmed that energy of nB_u is linear in U. Once again, these two observations indicate that nB_u is the lowest "band" state, while all states below it are excitonic.

To summarize, the calculated EA is remarkably similar to the experimental spectrum in that only two prominent signals are obtained. The high-energy EA is due to nB_u and immediately neighboring states, i.e., both A_g and B_u states at the band threshold contribute to the EA. The

state nB_u forms the lower threshold of the conduction band, as is indicated by these calculations. It is therefore not a coincidence that the threshold energies for photoconductivity[13] and EA are the same. Our earlier work[14] showed that THG is dominanted by the mA_g, whose energy lies in between the $1B_u$ and $2B_u$. Current work shows that EA is dominated by nB_u, where $n > 2$, and that nB_u also has a strong dipole moment with mA_g. THG and EA, therefore, give complementary information regarding locations of states. Based on these works, we show in Fig. 3 what we believe to be the locations of the most relevant energy states in the PDA's.

It is also appropriate to analyze the roles played by the excitonic A_g states that occur below the nB_u in EA. From Fig. 2(b), it would seem that the $2A_g$ (or any other A_g state below the $1B_u$) is weakly coupled to $1B_u$ and, thus, does not contribute to the EA spectra. This would be in agreement with recent experiments by Torruellas *et al.*[16] on a different PDA. The contribution of the mA_g to the EA spectrum is less clear. In the theoretical $\Delta\alpha$, the mA_g occurs as a peak in between the prominent $1B_u$ and nB_u signals for aribitrary U and V. In the experimental $\Delta\alpha$, an unusually large positive contribution is seen on the high-frequency side of the $1B_u$, slightly below the vibronic feature. It is, however, currently not possible for us to say whether this arises from simply the asymmetric shape of the $1B_u$ absorption line, or whether this is due to the mA_g. Clearly, further experimental work on the relative locations and strengths of the various two-photon states is required. While it has been suggested that the mA_g state is at a considerably higher energy,[17] it seems to us that the requirement that it has a strong dipole moment with both $1B_u$ and nB_u (and, therefore, is bound by these states) precludes this possibility.

Finally, we discuss the role of these very-high-energy states in third-order optical processes. It previously has been shown[14] that the channel $1A_g \rightarrow 1B_u \rightarrow mA_g \rightarrow 1B_u \rightarrow 1A_g$ gives most of the low-frequency third-order susceptibility, $\chi^{(3)}$. The band A_g and B_u states above the nB_u that are investigated here have very strong dipole moments among themselves but are weakly coupled to $1A_g$ or $1B_u$. On the other hand, the relatively large dipole moment between mA_g and nB_u indicates that a second channel $1A_g \rightarrow 1B_u \rightarrow mA_g \rightarrow nB_u \rightarrow 1A_g$ gives the remaining contributions to the total $\chi^{(3)}$. We have numerically confirmed that the four states, $1A_g$, $1B_u$, mA_g, and nB_u, give almost the entire $\chi^{(3)}$ and that no other significant states exist. The details of these results will be published elsewhere.

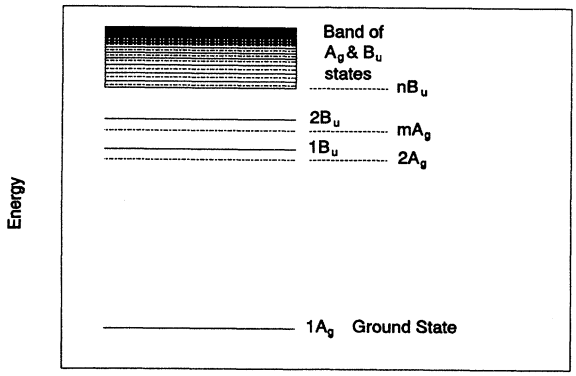

FIG. 3. Schematic representations of energy levels in a PDA. The band consists of closely spaced A_g and B_u states. The absolute energy spacings between the states are not known and are only schematically plotted. See the text for discussion of $2A_g$, mA_g, and nB_u.

The authors would like to acknowledge support from NSF (Grant No. ECS-89-11960) and the Optical Circuitry Cooperative of the University of Arizona. Work of S.N.D. was supported by U.S. DOE, Lawrence Livermore National Laboratory, under Contract No. W-7405-ENG-48. We wish to express our thanks to Mr. M. Pratt at Arizona State University for his preparation of the electrodes.

*Permanent address: Central Research Laboratories, Idemitsu Kosan Co., Ltd., 1280 Kamiizumi, Sodegaura, Chiba 299-02 Japan.

[1] *Nonlinear Optical Effects in Organic Polymers,* edited by J. Messier, F. Kajzar, P. Prasad, and D. Ulrich, NATO Advanced Study Institutes Ser. E Vol. 162 (Kluwer Academic, Dordrecht, 1989).

[2] P. D. Townsend, G. L. Baker, N. E. Schlotter, C. F. Klausner, and S. Etemad, Appl. Phys. Lett. **53**, 1782 (1988).

[3] M. Thakur and D. M. Krol, Appl. Phys. Lett. **56**, 1213 (1990).

[4] V. Williams, Z. Z. Ho, N. Peygambarian, W. M. Gibbons, R. P. Grasso, M. K. O'Brien, P. J. Shannon, and S. T. Sun, Appl. Phys. Lett. **57**, 2399 (1990).

[5] J. Le Moigne, A. Thierry, P. A. Chollet, F. Kajzar, and J. Messier, J. Chem. Phys. **88**, 6647 (1988).

[6] J. Le Moigne, A. Thierry, and F. Kajzar, in *Thin Films in Optics,* edited by T. Tschudi, SPIE Conference Proceedings No. 1125 (International Society for Optical Engineers, Bellingham, WA, 1989), p. 9.

[7] D. Baeriswyl, D. K. Campbell, and S. Mazumdar, in *The Physics of Conducting Polymers,* edited by H. Kiess (Springer-Verlag, Berlin, 1991), review article.

[8] L. Sebastian and G. Weiser, Phys. Rev. Lett. **46**, 1156 (1981).

[9] L. Sebastian and G. Weiser, Chem. Phys. **62**, 447 (1981).

[10] Y. Tokura, Y. Oowaki, T. Koda, and R. H. Baughman, Chem. Phys. **88**, 437 (1984).

[11] Y. Tokura, T. Koda, A. Itsubo, M. Miyabayashi, K. Okuhara, and A. Ueda, J. Chem. Phys. **85**, 99 (1986).

[12] D. N. Batchelder, in *Polydiacetylenes,* edited by D. Bloor and R. R. Chance, NATO Advanced Study Institutes Ser. E Vol. 102 (Martinus Nijhoff, Dordrecht, 1985), pp. 187–212, and references therein.

[13] K. Lochner, H. Bassler, B. Tieke, and G. Wegner, Phys. Status Solidi (b) **88**, 653 (1978), and references therein.

[14] S. N. Dixit, Dandan Guo, and S. Mazumdar, Phys. Rev. B **43**, 6781 (1991).

[15] B. E. Kohler and D. E. Schilke, J. Chem. Phys. **86**, 5214 (1987).

[16] W. E. Torruellas, K. B. Rochford, R. Zanoni, S. Aramaki, and G. I. Stegeman, Opt. Commun. **82**, 94 (1991).

[17] Z. G. Soos, P. F. McWilliams, and G. W. Hayden, Chem. Phys. Lett. **171**, 14 (1990).